6ICEGE 6th International Conference on Earthquake Geotechnical Engineering
1-4 November 2015
Christchurch, New Zealand

Large Scale Testing of Shallow Ground Improvements using Blast-Induced Liquefaction

F.J. Wentz[1], S. van Ballegooy[2], K.M. Rollins[3], S.A. Ashford[4] and M.J. Olsen[5]

ABSTRACT

To increase the resilience of new/rebuilt houses in Christchurch, the New Zealand Earthquake Commission (EQC) funded a study to evaluate the use of shallow (i.e., ≤ 4 m deep) ground improvements to construct a stiff, non-liquefiable crust. This paper presents the methodology used for the blast testing, and summarises some of the more significant findings from the overall blast testing program. This effort included large-scale testing of several ground improvement methods using controlled blasting to induce liquefaction to depths of 10 to 12 m beneath the zone of improvement. The blast-induced liquefaction testing demonstrated that ground surface differential settlement generally increases with increasing total settlement and that improvements that formed stiffer crusts experienced less structurally damaging differential settlement.

Introduction

The 2010 – 2011 Canterbury Earthquake Sequence (CES) caused widespread liquefaction related land and building damage, affecting 51,000 residential properties in Christchurch, including 15,000 residential houses damaged beyond economical repair. Most damage occurred from differential settlement induced by liquefaction. Specifically, differential settlement comprised of flexural distortion or "curvature" resulted in significantly greater foundation/structural damage than did rigid tilt. Damage observations and geotechnical assessments of approximately 60,000 residential properties clearly demonstrated that almost no foundation deformation occurred in areas with liquefaction susceptible soils overlain by an intact, relatively stiff, non-liquefying crust with a minimum thickness of approximately 3 m. This finding is consistent with those of Ishihara (1985) who recognised that a thick and/or stiff non-liquefiable crust can reduce the consequences of liquefaction (i.e., sand boils, loss of bearing capacity and differential settlement). To increase the resilience of new/rebuilt houses on vulnerable land, the New Zealand Earthquake Commission (EQC) funded a comprehensive study to evaluate the efficacy and technical viability of using shallow ground improvement (i.e., < 4 m) to reduce liquefaction vulnerability for the rebuild and repair of houses. The methods tested included Rapid Impact Compaction (RIC), Rammed Aggregate Pier™ (RAP) reinforcement, Driven Timber Piles (DTP), Low Mobility Grout (LMG), Resin Injection (RES), Gravel Rafts (GR), Soil Cement Rafts (SCR) and Horizontal Soil-cement Mixed (HSM) beams. The construction methodology of each of the tested ground improvement methods is described in van Ballegooy et al. (2015b).

[1]Principal, Wentz-Pacific Ltd., Napier, New Zealand, rwentz@wp-geo.co.nz
[2]Senior Geotechnical Engineer, Tonkin & Taylor Ltd., Auckland, New Zealand, svanBallegooy@tonkin.co.nz
[3]Professor, Dept. of Civil & Env. Eng., Brigham Young Univ., USA, rollinsk@byu.edu
[4]Professor, School of Civil & Const. Eng., Oregon State Univ., USA, scott.ashford@oregonstate.edu
[5]Asst. Prof. Michael Olsen, Sch. of Civil & Const. Eng., Oregon State Univ.,USA, michael.olsen@oregonstate.edu

The construction methodology of the HSM beams is presented in detail in Hunter et al. (2015).

Test panels for each ground improvement method were constructed at three sites in Christchurch in areas severely affected by liquefaction (see Wissmann et al., 2015 for more details). The testing phase comprised pre- and post-improvement Cone Penetration Testing (CPT) and crosshole pressure wave velocity (V_P) and shear wave velocity (V_S) testing, vibroseis T-Rex testing, and blast-induced liquefaction testing. The CPT, crosshole V_P and V_S testing and T-Rex shake test results are presented in van Ballegooy et al. (2015a) and Wissmann et al. (2015). The purpose of this paper is to describe the methodology and results of the blast-induced liquefaction testing, which was undertaken at only one of the test sites (Site 4, Wissmann et al. 2015).

The aim of the large scale blast testing was to induce liquefaction below the various ground improvements to obtain a direct comparison of system performance after treatment. Performance was evaluated in terms of a method's ability to control structurally damaging liquefaction-induced differential settlement (and hence increase post-earthquake resilience). While it is recognised that blast-induced liquefaction is mechanistically different from liquefaction caused by an earthquake, the scale and behaviour of the liquefied soil was similar enough to allow assessment of the performance of the tested ground improvements. Three practice blasts were conducted to optimize the charge sizes and layouts, followed by seven production blasts to test the ground improvement methods. This paper focusses on the methodology and findings from production blast 5 (PB5); however, the analysis and conclusions herein are drawn from the results of the entire EQC blast testing program.

PB5 included 4 test panels: 1) a 1.2 m thick SCR; 2) a 1.2 m thick geogrid-reinforced compacted GR; 3) a double-row of HSM beams; and 4) Natural Soil (NS). A specific objective of PB5 was to produce a significant amount of liquefaction ejecta over the blast area to more closely replicate (relative to the first 4 production blast tests) the observed liquefaction manifestations caused by the CES. However, the design of the blasting procedure and layout also needed to achieve a delicate balance between: 1) generating enough energy to induce sufficient liquefaction for a sustained period of time to reasonably replicate the liquefaction-related ground surface manifestations caused by earthquakes; 2) minimising excessive vertical acceleration at the ground surface, which could cause ground heave / lurch and adversely affect settlement measurements used to compare the relative performance of the ground improvement methods; and 3) minimising detrimental vibration effects in neighbouring occupied suburbs.

Subsurface Conditions, Test Panel and Charge Layout and Blasting Methodology

The test panel locations, associated charge layouts and subsurface investigations are shown in Figure 1. Ten CPT and three crosshole V_P and V_S tests were conducted across the test site to characterize the subsurface conditions. The subsurface soils at the test site consisted of approximately 2 m of loose silt/sandy silt overlying generally loose to medium dense silty sand/sand. Relatively clean, predominantly medium dense sand was consistently present below a depth of about 4 m across the test site. The CPT and crosshole V_S data from the test site are shown in Figure 2. The two highlighted CPT traces encountered siltier soil layers within the test site based on the Soil Behaviour Type Index (I_c) values. The depth to groundwater was approximately 1.2 m and fluctuated daily in the order ± 300 mm, in sync with the tidal influence

in the nearby river. The depth to full saturation, based on the results of the crosshole V_p testing, was approximately 2 to 3 m.

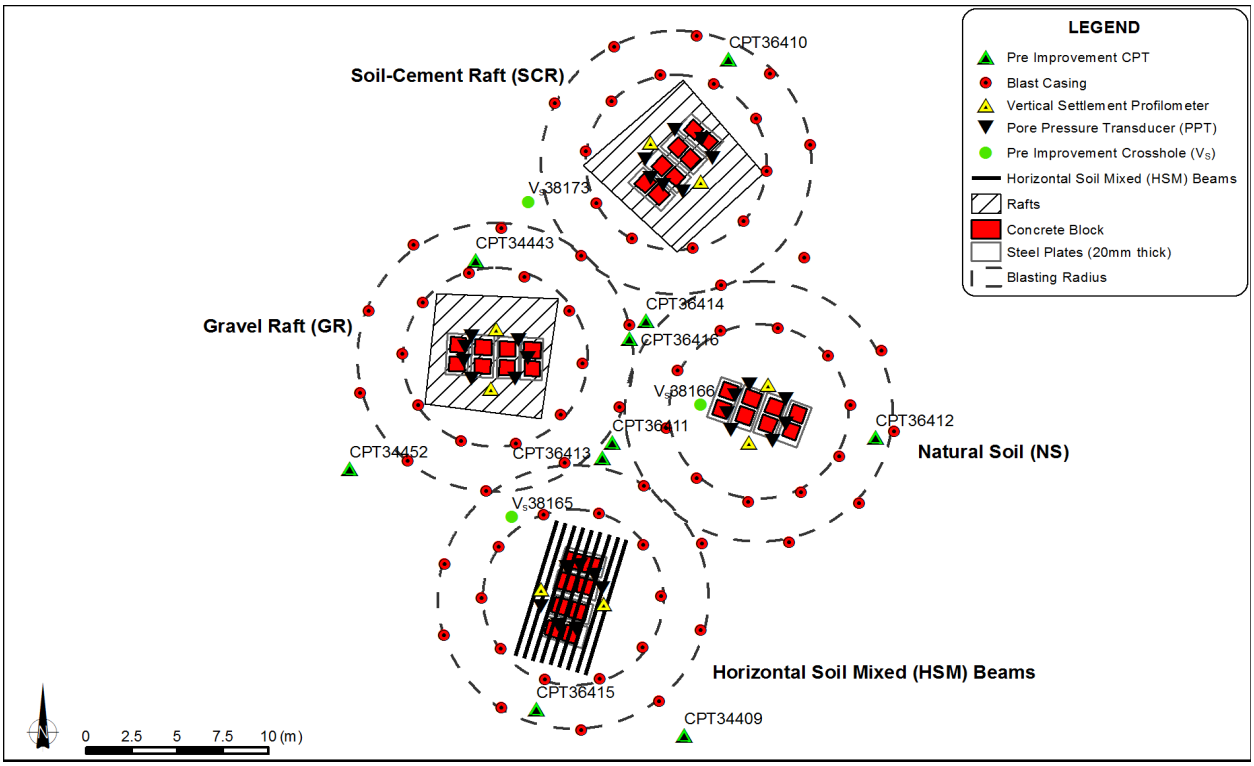

Figure 1: Test panel locations and subsurface investigation, instrumentation and charge layouts.

Symmetrical charge layouts were used to ease the interpretation of the results. Double rings of charges were installed in blast casings around each test panel; an inner 10 m diameter ring and larger outer 15 m diameter ring. Ten blast casings were evenly spaced around the perimeter of each ring (at approximately 3.1 m centre-to-centre spacing). The outer ring casings were horizontally offset from the casings on the inner rings in order to achieve a minimum 3 m horizontal distance between all charges (to avoid charges in adjacent casings from detonating each other). The blast casings comprised 12 m long, 80 mm diameter PVC pipe installed through steel casing using rotary-sonic drilling techniques. The casing was vibrated out of the ground to collapse the borehole and fill the annulus between the borehole wall and casing. The annulus in the upper 2 m of each hole was filled with cement-bentonite grout seal. Each blast casing contained three levels or "decks" of gelignite charges as shown in Figure 2. A total of 396.8 kg of explosives were distributed around the 4 test panels. Angular roading chip gravel (approximately 5 mm dia.) was used to fill each blast casing up to the depth of the base of the bottom charge, then around the charges and up to the ground surface. The tops of the casings were covered with blast mats and sand bags.

To reduce potential vibration effects on nearby structures, three detonation sequences were planned in order to spread out the release of energy over a 30 s period. The concept was to detonate the bottom and middle decks of the inner blast rings first in order to liquefy the soil

beneath the test panels, followed in rapid succession by detonation of the bottom and middle decks of the outer blast rings to further liquefy the surrounding soil in order to maintain the excess pore water pressure ratio, r_u, and increase the duration of liquefaction. The top decks of charges in the inner and outer rings were detonated last to liquefy the shallow soil layers and fracture the crust.

Test Panel Surcharge and Instrumentation and Lidar Ground Surveys

Instrumentation of the test panels included GE-Druck UNIK 5000 Pore Pressure Transducers (PPTs), vertical settlement profilometers (Sondex Settlement System by Slope Indicator) and surface and subsurface geophones. Only the results from the PPTs and profilometers are discussed in this paper. The locations of the instrumentation in each test panel is shown in Figure 1 and the depth of the PPTs are shown in Figure 2. Seven PPTs were installed in each test panel around an approximately 3 m diameter instrumentation ring located at the centre of the panel, at depths of approximately 2, 3, 4, 5, 7, 9 and 11 m below the ground surface. Two profilometers were installed on opposite sides of the instrumentation ring to assess where in the soil profile the liquefaction-induced settlement occurred. The profilometers were installed to a depth of 14 m. The minimum horizontal distance between the profilometers and the PPTs was 1 m.

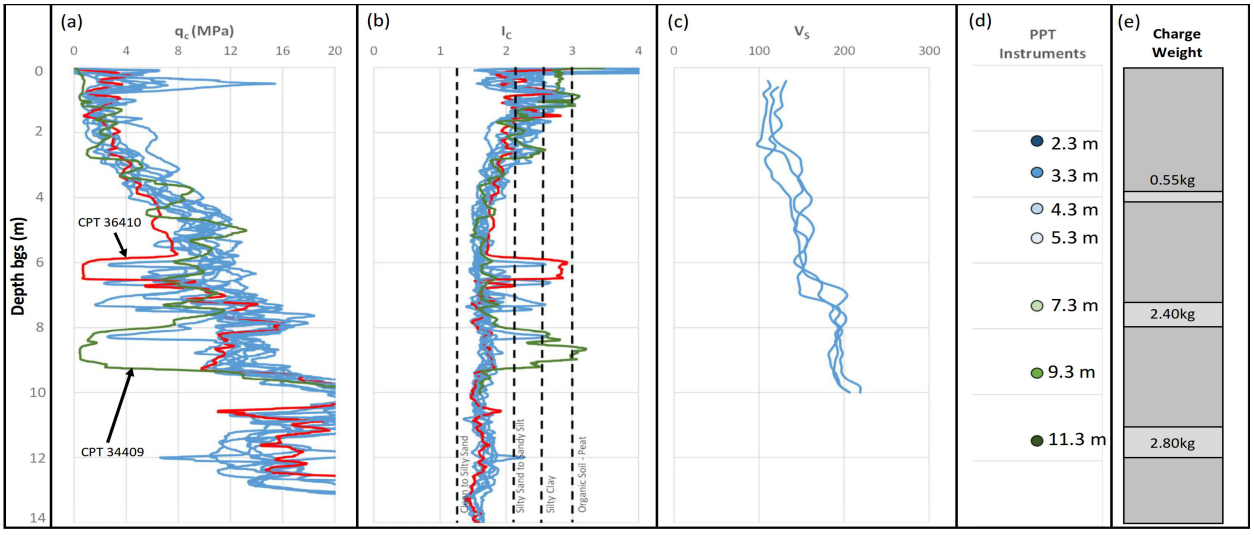

Figure 2: CPT and Crosshole VS data from test site and locations of PPTs and gelignite charges.

A surcharge was placed on each test panel to simulate an applied load. The surcharge comprised four 20 mm x 1.2 m x 2.4 m steel plates set side by side in a rectangular pattern with two 1 m^3 concrete blocks placed on top of each plate. The plates were used to evenly distribute the weight of the concrete blocks, and a 100 mm gap was left between adjacent plates to allow them to move independently during post-blast settlement. The total weight of the plates/blocks divided by a 2.4 x 5.1 m area equates to about a 16 kPa surcharge. The relative elevations of the four corners and centre of each steel plate were measured before and after blasting using an optical level mounted on a tripod located well outside of the test area.

Ground-based Lidar (GBL) and total station surveys were conducted before and after each blast test to capture the post-blast ground deformations. Each survey consisted of 8 to 15 setups distributed across the site to minimize occlusions from obstructions. The relative accuracy of the surveys was estimated as +/-10 mm (3D root mean squared). Digital Elevation Models (DEMs) with 2 cm resolution were generated from the pre- and post-blast surveys and differenced to analyse the spatial variability of the settlement. Total station surveys captured stable control points, lidar reference targets, sand boils, and profilometers elevations, to confirm whether the entire profilometer had moved, due to liquefaction beneath it, as had happened in earlier tests.

Results of the Blast Testing

During the initial detonation sequence (of the three planned), a detonation wire to one of the charges in the second sequence was damaged. This tripped a safety switch and prevented firing of the second and third sequences immediately after the first sequence. The second sequence was detonated 4 minutes after the detonation of the first sequence. By the time the electronics for the third sequence (i.e., the top deck of charges) were reset and ready for firing, 90 minutes had elapsed from the time of the first blast. Detonation of the third sequence was deferred to the following day to allow sufficient time to complete a round of post-blast instrumentation monitoring and lidar survey to measure the liquefaction related ground surface subsidence caused by the detonation of the lower and middle decks of the charges. The remainder of this discussion focusses on the results from the first two detonations. The two blasts produced significant liquefaction ejecta and ground surface settlement; both within and beyond the blast rings. Figure 3 presents plots of r_u with time for all PPTs located beneath the four test panels. A r_u value of 1 (full liquefaction) was reached in all but the two shallowest PPTs (2.3 m deep) located in the NS and SCR test panels. These PPT were located within siltier soils and the higher fines content may have inhibited the full build-up of excess pore pressure. Values of r_u were computed assuming a bulk saturated soil density of 18 kN/m^3. The excess pore water pressure measured in the shallower PPTs increased during the dissipation phase (post blasting), indicating an upward flow of water from the underlying liquefied soils. Figure 3 indicates that r_u values at greater depths decreased more rapidly than those at shallower depths, also indicating an upward flow of water.

Approximately two minutes after the second blast, water and sand (liquefaction ejecta) flowed out of the ground at discrete locations for up to 30 minutes. The mapped locations of sand ejecta are shown in Figure 4. The duration of surface flow was consistent with the duration of sustained excess pore pressure measured by the PPTs. Notably larger amounts of water ejecta and some sand ejecta occurred on the southern end of the blast area (near the HSM beam test panel). In comparison, there was notably less water ejecta and very little sand ejecta across the northern portion of the blast area (around the SCR test panel). The ejected fine grey sand was typical of the soil material encountered below a depth of 2 to 3 m across the entire test site, and was the same (in terms of colour, texture and grain size) as the soil ejected during the CES.

Figure 4 shows the change in ground surface elevation after the blast test, along with summary tables of the 15th, 50th and 85th percentiles of settlement values for each test panel (7 x 7 m area) and corresponding central surcharge zone (4 x 4 m area). The settlement patterns are relatively symmetrical for 3 of the 4 test panels; ranging from little settlement at a horizontal distance of 5

m from the outer perimeter of blast casings, to about 130 to 250 mm in the centre of the test panels. The total settlement of the SCR test panel was less than that of the other three test panels (Figure 4). The highlighted red trace of I_c values for CPT 36410 in Figure 2 indicates that a layer of silty to very silty soil (approximately 1 m thick) was present at a depth of about 6.5 m beneath the SCR test panel. In general, the soils beneath the SCR test panel also contain more silt than those beneath the three adjacent test panels. A reduction in liquefaction-induced settlement beneath the SCR as a result of the higher silt content helps explain the pattern of settlements shown in Figure 4. The profilometer settlement data (Figure 3) indicates that for 3 of the 4 test panels, the majority of the settlement occurred over the depth interval between approximately 1.5 and 7.5 m.

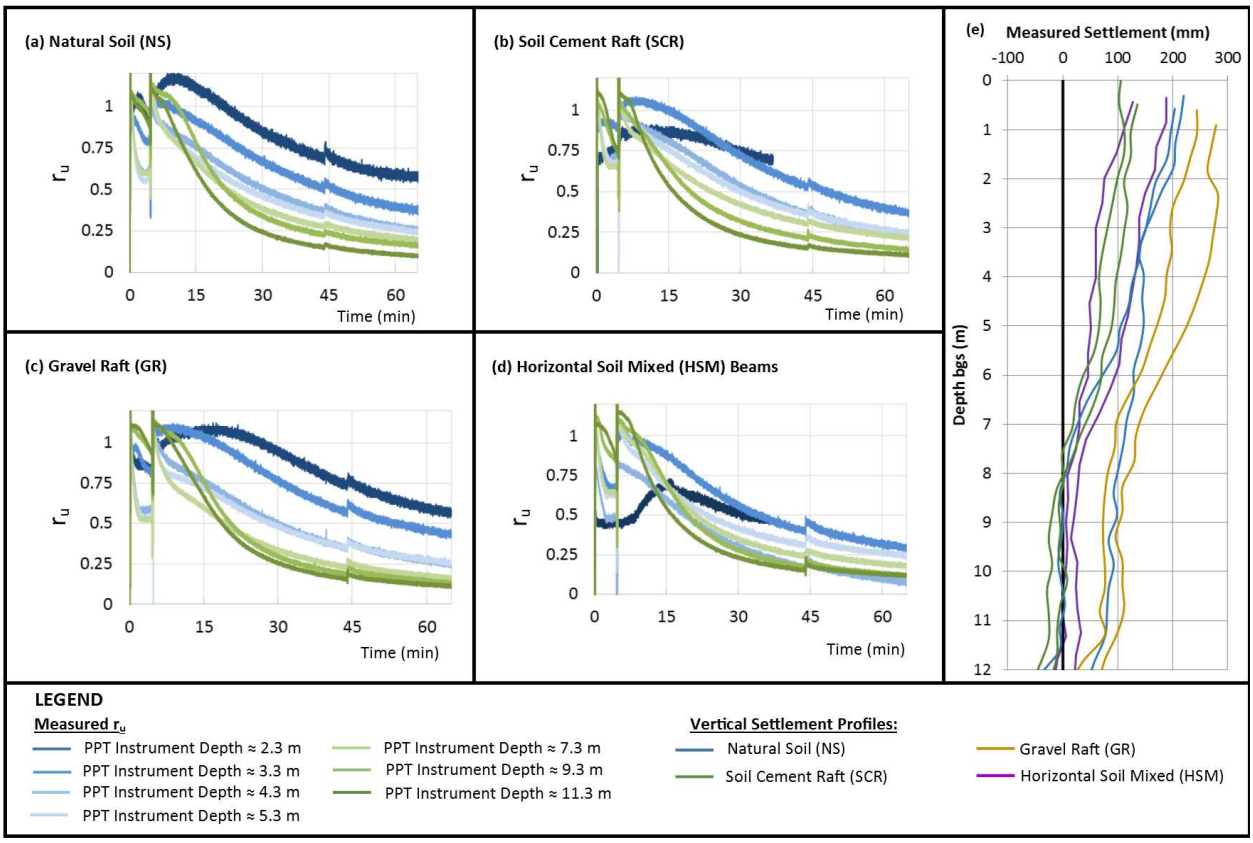

Figure 3: Excess pore pressure ratio r_u vs time and vertical settlement data for each test panel.

Analysis of the Results, Discussion, and Conclusions

The following discussion considers test data from all of the production blast tests. The blast-induced liquefaction settlement of the 17 test panels included in the study was compared to the predicted earthquake-induced one-dimensional post-liquefaction reconsolidation settlement (S_{V1D}) for the 25, 100 and 500 year return period design ground motions as specified in the MBIE (2012) guidance, which represent a M 7.5 earthquake and peak ground accelerations (PGAs) of 0.13g, 0.20g and 0.34g, respectively. This comparison provides insight into the equivalent level of earthquake shaking required to generate a liquefaction demand similar to that

created by the blasts. The pre- and post-improvement liquefaction triggering/settlement analyses (Figure 5d) were performed utilising the CPT-based procedures by Idriss and Boulanger (2008) and Zhang et al. (2002). Also shown are the measured 15th, 50th and 85th percentiles of the blast-induced total settlement values for each panel (sampled from the 7 x 7 m area in the centre of each blast ring). It can be seen that the measured settlements resulting from PB5 are, in general, larger than the settlement (S_{V1D}) predicted to result from the 500 year return period earthquake scenario.

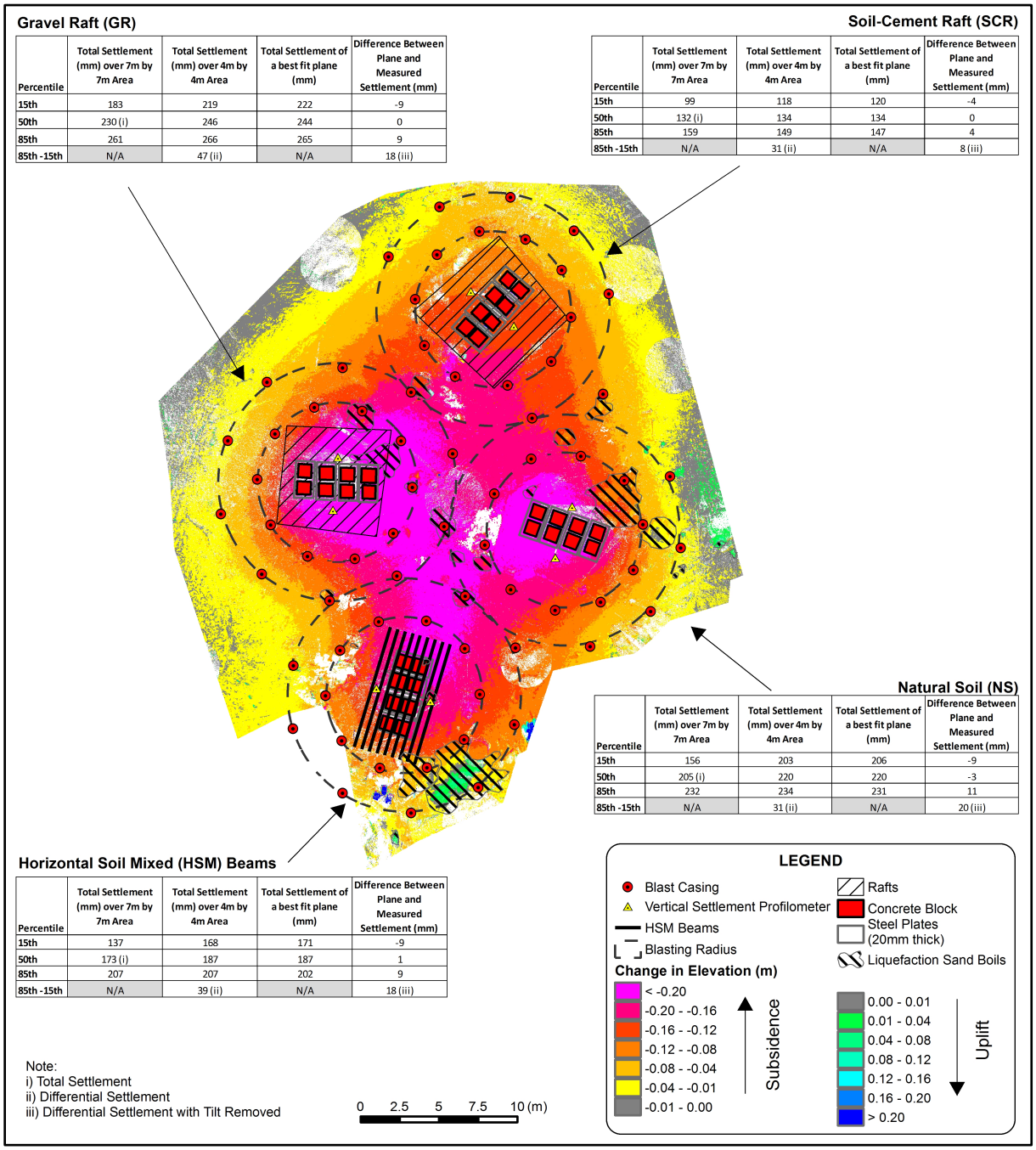

Gravel Raft (GR)				
Percentile	Total Settlement (mm) over 7m by 7m Area	Total Settlement (mm) over 4m by 4m Area	Total Settlement of a best fit plane (mm)	Difference Between Plane and Measured Settlement (mm)
15th	183	219	222	-9
50th	230 (i)	246	244	0
85th	261	266	265	9
85th -15th	N/A	47 (ii)	N/A	18 (iii)

Soil-Cement Raft (SCR)				
Percentile	Total Settlement (mm) over 7m by 7m Area	Total Settlement (mm) over 4m by 4m Area	Total Settlement of a best fit plane (mm)	Difference Between Plane and Measured Settlement (mm)
15th	99	118	120	-4
50th	132 (i)	134	134	0
85th	159	149	147	4
85th -15th	N/A	31 (ii)	N/A	8 (iii)

Natural Soil (NS)				
Percentile	Total Settlement (mm) over 7m by 7m Area	Total Settlement (mm) over 4m by 4m Area	Total Settlement of a best fit plane (mm)	Difference Between Plane and Measured Settlement (mm)
15th	156	203	206	-9
50th	205 (i)	220	220	-3
85th	232	234	231	11
85th -15th	N/A	31 (ii)	N/A	20 (iii)

Horizontal Soil Mixed (HSM) Beams				
Percentile	Total Settlement (mm) over 7m by 7m Area	Total Settlement (mm) over 4m by 4m Area	Total Settlement of a best fit plane (mm)	Difference Between Plane and Measured Settlement (mm)
15th	137	168	171	-9
50th	173 (i)	187	187	1
85th	207	207	202	9
85th -15th	N/A	39 (ii)	N/A	18 (iii)

Figure 4: Summary of measured ground surface settlement at each test panel.

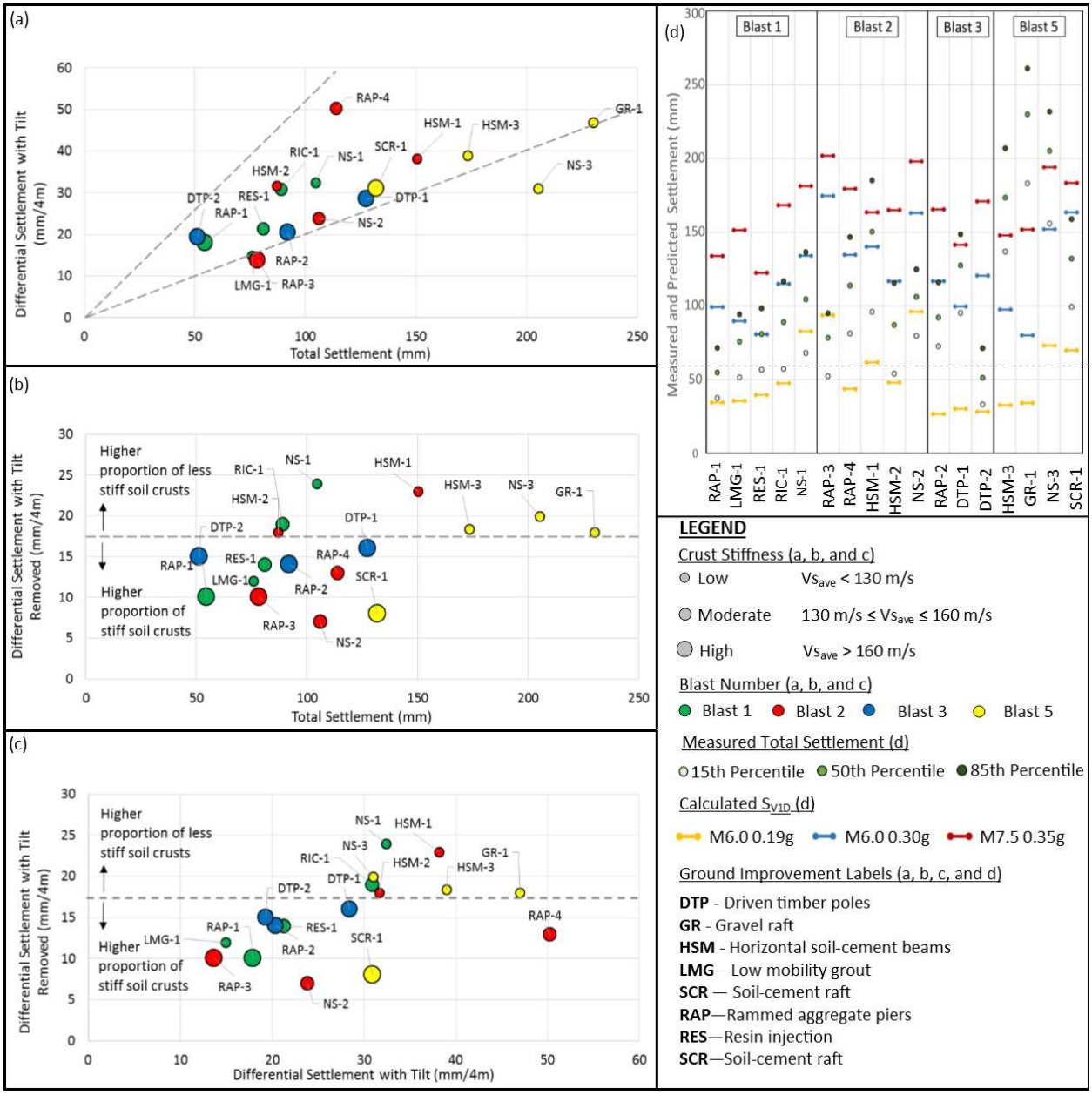

Figure 5: (a) Differential settlement vs total settlement, (b & c) differential settlement with tilt removed vs total settlement and differential settlement, respectively, and (c) liquefaction settlement compared with predicted CPT-based volumetric strain calculated settlement (S_{V1D}).

Figures 5b and 5c show that the test panels with relatively stiffer shallow ground improvements (i.e., stiffer non-liquefiable crusts measured by the crosshole V_S testing), the amount of differential settlement with tilt removed was notably less than for those with relatively less stiff improvements. These results indicate that the stiffness of the surface crust should be considered in addition to the thickness as originally proposed by Ishihara (1985).

Some of the ground improvement test panels had greater total settlement than others due to the variability of soil conditions across the test site and the resulting spatial variation of the development of excess pore water pressures induced during blast testing. Some test panels performed well in limiting the differential settlement of the supported surcharge even though they underwent larger total settlements. Likewise, some of the test panels did not perform well in limiting the distortion of the supported surcharge even though smaller total settlement occurred.

Therefore, in order to appropriately evaluate the performance of the ground improvements under blast-induced liquefaction, it was necessary to express the differential settlement of the test panels in terms of flexural distortion; specifically, the deviation from planar tilt. To do this, a best fit plane was fitted to the surface settlement profile over a 4 x 4 m area in the centre of each test panel with the tilt component removed from the differential settlement. The tilt-removed differential settlement of the test panels was calculated as the 85^{th} percentile of the measured settlement with the tilt removed minus the 15^{th} percentile of the measured settlement with the tilt removed.

The calculated differential settlement and differential settlement with tilt removed for each test panel is plotted against the total measured blast-induced settlement in Figures 5a and 5b (yellow dots represent results from PB5). Also plotted (Figure 5c) is the differential settlement with tilt removed vs differential settlement with tilt. Figure 5a shows that as the amount of measured blast-induced total settlement increased, the differential settlement also increased. This is an expected outcome; however, the ratio of differential settlement to total settlement ranged between 0.2 and 0.5.

In summary, the controlled use of large-scale blast testing was found to be a useful tool to assess the performance of various shallow ground improvements in mitigating the effects of liquefaction. The blasting was shown to generally replicate the liquefaction demand predicted to occur as a result of the target levels of earthquake ground shaking. This was demonstrated through the use of a robust instrumentation program to measure excess pore pressure development, ground surface settlement and layer specific settlement within the soil profile.

Acknowledgments

The experimental work described in this paper was funded by the New Zealand Earthquake Commission. This support is gratefully acknowledged. The authors would also wish to acknowledge H. Cowan and K. Yamabe from the Earthquake Commission. The authors appreciate the assistance of the numerous individuals involved in the testing.

References

Hunter, R., van Ballegooy, S., Leeves, J., & Donnelly, T. (2015). Development of horizontal soil mixed beams as a shallow ground improvement method beneath existing houses. *Proceedings of the 12th Australia New Zealand Conference on Geomechanics* (pp. 650-657). Wellington, New Zealand: NZGS and AGS.

Idriss, I. M., & Boulanger, R. W. (2008). *Soil liquefaction during earthquakes.* Earthquake Engineering Research Institute. Oakland, CA: Monograph MNO-12, pp. 261.

Ishihara, K. (1985). Stability of natural deposits during earthquakes. *Proceedings of the 11th International Conference on Soil Mechanics and Foundation Engineering*, *1*, pp. 321-376. San Francisco.

MBIE. (2012). *Repairing and rebuilding houses affected by the Canterbury earthquakes.* Ministry of Business, Innovation and Employment. December 2012. Retrieved from http://www.dbh.govt.nz/guidance-on-repairs-after-earthquake

van Ballegooy, S., Roberts, J., Stokoe, K., Cox, B., Wentz, F., & Hwang, S. (2015a). Large scale testing of ground improvements using controlled, dynamic staged loading with T-Rex. *Proceedings of the 6th International Conference on Earthquake Geotechnical Engineering.* Christchurch, New Zealand: ISSMGE.

van Ballegooy, S., Wentz, F., Stokoe, K., Cox, B., Rollins, K., Ashford, S., & Olsen, M. (2015b). *Christchurch Ground Improvement Trial Report.* Report for the New Zealand Earthquake Commission. (In press).

Wissmann, K., van Ballegooy, S., Metcalfe, B., Dismuke, J., & Anderson, C. (2015). Rammed aggregate pier ground improvement as a liquefaction mitigation method in sandy and silty soils. *Proceedings of the 6th International Conference on Earthquake Geotechnical Engineering.* Christchurch, New Zealand: ISSMGE.

Zhang, G., Robertson, P., & Brachman, R. (2002). Estimating liquefaction-induced ground settlements from CPT for level ground. *Canadian Geotechnical Journal, **39***(5), 1168-1180.